7th International Building Physics Conference

IBPC2018

Proceedings

SYRACUSE, NY, USA

September 23 - 26, 2018

Healthy, Intelligent and Resilient
Buildings and Urban Environments

ibpc2018.org | #ibpc2018

Experimental Study of the Performance of a Double Skin Façade Window under Non-Solar Conditions

Jiayi Zhu, Guoqing He*, Qihuan Luo and Yu Liu

College of civil engineering and architecture Zhejiang University Hangzhou China

**Corresponding email: guoqinghe@zju.edu.cn*

ABSTRACT
This paper reports measured heat transfer coefficient of a double skin façade (DSF) window measured 1.1 m by 0.7 m at varied depth in the absence of solar radiation using a calorimeter box. The results showed that the DSF had better insulation than the double glazing especially with cavity closed. All the studied factors (ventilation, cavity width, and outdoor temperature) had influence on the heat transfer coefficient and such influence could be season specific. Measurements confirmed the existence of an optimal width in winter for best insulation.

KEYWORDS
Double skin façade, U value, experiments, non-solar radiation

INTRODUCTION

Double skin façades (DSFs) have received increasing attention in research and in practice since their first appearance in northern Europe (Poirazis 2006). In addition to its freedom in aesthetic expression, the cavity between the two layers offers potential energy savings (Ghaffarianhoseini et al., 2016) and even carbon reduction in a life cycle (Pomponi and D'Amico, 2017). Recent studies explored the performance of varied forms of DSFs, such as phase change material attached blinds (Li et al., 2017), photovoltaic (PV) panel attached blinds (Kapsis and Athienitis, 2015; Luo et al., 2017), fan-coil combined DSF design (Bueno et al., 2017), and pipe-embedded DSF design (Shen and Li, 2016). These studies attempted to make the best of the double layers, which protect solar shading devices and other materials from the outdoor environment while keeping the heat absorbed in the cavity outdoors.

What makes the DSF unique is thought to be the double layers and various ventilation schemes to meet different needs in different seasons, i.e., one design that can work in both cooling and heating seasons, suitable for regions such as the hot summer and cold winter zone in China. Such capability requires the DSF to have good insulation, good shading performance in summer, and good solar heat gain in winter. The installation of blinds and its combination with other new materials aim to meet the later two needs. The double layer structure typically consisting of a double glazing and a single pane presumably provide better insulation than a normal double glazing, whose U values are typically around 2.80 W/m^2/K. There are limited studies on the U values of DSFs. Recent studies have defined the U value of a DSF window based on total heat transferred through inner surface excluding the direct solar transmittance (here referred as heat transfer based U value, or U_{HT}). Luo et al. (2017) reported experimental data of U_{HT} as 2.2 to 2.8 W/m^2/K for naturally ventilated DSFs, lower than 3.8 W/m^2/K reported by Peng (Peng and Lu et al., 2015) for a naturally ventilated DSF with a semi-transparent PV film attached to the outer pane. Note that U_{HT} is not comparable to the conventional U value defined based on steady state heat transfer without solar radiation because the former includes part of the absorbed solar irradiation on the inner pane of the window which then enters into the room as heat gain by convection or irradiative heat transfer.

Chow et al. (2010) and He et al. (2016) used a different approach where total room heat gain of a window is expressed as a linear function of solar irradiation and the temperature difference between the room and the outside, which is confirmed by experiment in the case of DSF (He et al., 2016). The coefficient of the temperature term is defined as the U value (room heat gain based U value, or U_{HG}), which is difficult to measure directly. For common double glazing, Chow et al. (2010) showed that the calculated values of U_{HG} are close to the typical U values. For DSF, He et al. (2016) determined the U_{HG} value of a DSF window together with the solar shading coefficient by fitting the experimental data. However, the contribution of heat transfer through the DSF was shadowed by the solar radiation, making it difficult to obtain a U value with meaningful certainty. Nevertheless, their simulations indicated that the U value of DSF windows could be significantly lower than that of the corresponding double glazing indicating improved insulation by the addition of an extra layer.

Previously discussed U values of DSFs reflects the overall heating transfer coefficient in the present of solar radiation. To our best knowledge, there have not been any studies on the U value of DSF in the absence of solar radiation (conventional U values). Given the amount of non-solar time in a day, the conventional U value of the DSF is critical to the performance of DSF. This paper attempts to fill this gap by studying the conventional U value of a DSF window experimentally.

METHODS

Experiment setup

Experiments were carried out indoors with the same DSF model and calorimeter described in He et al. (2016). The model box was 1.3 m × 1.1 m × 0.88 m (Figure 1) and consisted of a small version of DSF window on one wall. All other three walls, floor and ceiling were 0.1 m thick extruded polystyrene (XPS) panels, each covered by a thin (0.005 m) aluminum sheet outside. The outer layer of the DSF window was a single-pane glazing and the inner layer was a double glazing. All glazing panes were clear float glasses. There were two openings of equal height (0.02 m) at the top and the bottom of the single pane glazing. The double glazing separates the box into two spaces: the cavity of the DSF and the test chamber. By moving the double glazing, the distance between the single pane and the double glazing can be changed. An aluminum micro-channel heat exchanger was used as the heating source with the water flowed in from the bottom and out from the top. Inflow temperature was maintained constant at a desired value by a water bath. The pipe for connection is PPR (Polypropylene-Random, ϕ20mm) tube insulated using rubber foam. A rotameter (±2.5%) was used to measure the flow rate and its accuracy was checked by measuring the volume of the water at a given time.

In total, T-type thermocouples were used to measure temperatures of the aluminum plate (5 sets), double glazing (3 sets), single pane (1 set), room air (1 set), cavity air (3 sets), and test chamber air (6 sets), inflow water (1 set), and outflow water(1 set). For room air temperature measurement, a cup-shaped aluminum foil surrounded the thermocouple to reduce the radiative heat transfer from indoor environment. All thermocouples were calibrated against a platinum resistance thermometer (previously calibrated to 0.1 °C accuracy by the Center of Cryogenic Metrology in Chinese Academy of Sciences) in the range of -20 to 100 °C. The calibration results were used to correct the measured temperature to an accuracy of 0.2 K. Temperatures were recorded every 10 seconds using two data acquisition modules (NI 9213 and NI 9219).

Air velocity was measured at three positions (A, B, C) using thermal anemometers (Swema 03, 0.05~ 10 m/s, ±0.04 m/s or ±4%). Position A is 30cm above the top surface of the test chamber. Position B was 10 cm away from the center of the front glazing pane. Point C was used to measure the air speed inside the cavity at the bottom but 10cm from the opening.

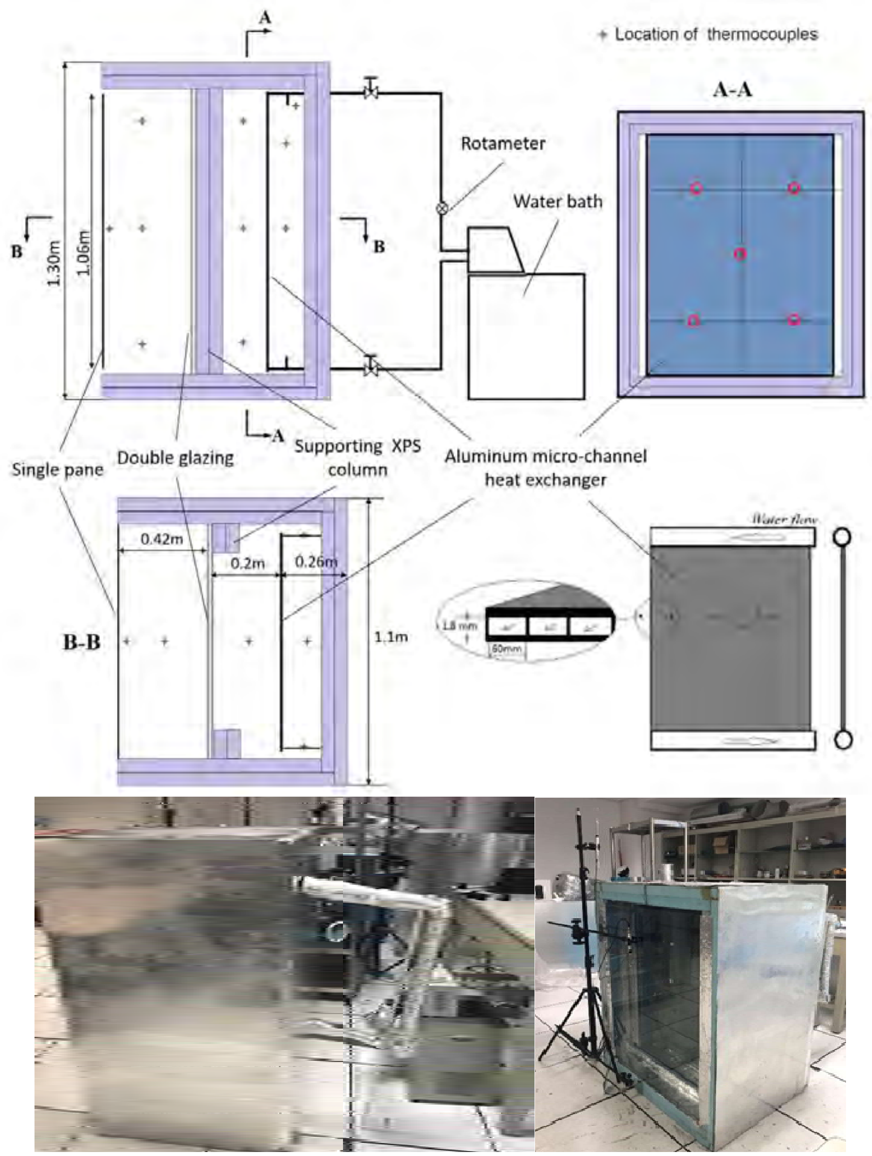

Figure 1. Sketches and photos of the DSF system and the location of measuring point

Determination of heat transfer coefficients

The energy change in the water flow from the inlet to the outlet is balanced by the heat transfers through the DSF and the envelope.

$$c_p(T_{in} - T_{out})q = u_{DSF}A_{DSF}(T_r - T_a) + u_0 A_0 (T_r - T_a) \quad (1)$$

where $c_p$is the specific heat of the water. T_{in} and T_{out} are the inlet and outlet temperatures, respectively. q is the mass flow rate. u_{DSF} is the overall heat transfer coefficient of DSF window and u_0 is the heat transfer coefficient of the XPS walls and needs to determined separately. A_{DSF} is the area of the DSF and A_0 is the inner surface area of the envelope. T_r and T_a is the temperature of the chamber air and the room air, respectively.

The last term in Equation 1 is the heat loss through the XPS walls of the envelope. To determine u_0, the single glaze pane was removed and the double glazing was covered by two 50 mm thick XPS plates on both sides. With this modification, the heat input by the water is assumed to be balanced by the heat loss through the XPS walls only. u_0 is determined by Eq. (1) with u_{DSF} being replaced by u_0 .

RESULTS AND DISCUSSION

Heat transfer coefficient of the XPS walls

The heat transfer coefficient of the XPS walls (u_0) was measured at three different temperature differences (T_r -T_a), each repeated at least 12 times (Figure 2). The standard deviations were less than 10% of the heat transfer coefficients indicating good repeatability. u_0 increased with the temperature difference. This is reasonable as larger temperature difference means stronger buoyancy force and convection on both sides of the walls. For the range of temperature considered, the heat transfer coefficient u_0 could be correlated to the temperature difference using the following formula:

$$u_0 = 0.0193\ln(T_r - T_a) + 0.3391 \tag{2}$$

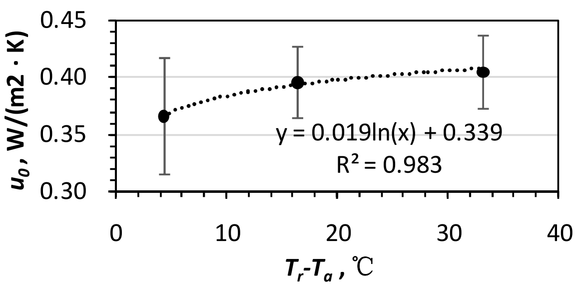

Figure 2. Plot of means and standard deviations of measured heat transfer coefficient of the XPS walls(u_0) at three temperature difference.

Although u_0 was determined in the heating mode, i.e., chamber air is hotter than the outside, it is assumed that it applies to the cooling mode as well, where chamber air is colder than the outside. u_0 can be converted to the conventional U value of the XPS walls if the convection coefficients on both sides of the wall can be determined. However this is irrelevant to the objective of this study.

Impact of cavity ventilation

In the non-ventilation mode, the upper and bottom openings of the outer pane were sealed using duct tape. Experiments were carried out under positive temperature difference and negative temperature difference, corresponding to the winter mode and summer mode, respectively. The range of the temperature difference covers the typical weather conditions in the hot summer and cold winter region of China. At least five repeat tests were conducted at each temperature difference and the results are shown in Figure 3. The repeat points are more clustered at higher temperature difference. In order to reach small temperature difference, the water flow rate had to be increased which resulted a small temperature drop from the inlet to the outlet. At 4 ^{o}C difference, the water temperature drop reduced to within 0.5 ^{o}C approaching to the uncertainty range of the temperature measurements, resulting greater uncertainties.

In either heating or cooling mode, the non–vented DSF had smaller u_{DSF} than the naturally ventilated DSF indicating better insulation. The measured u_{DSF} for the ventilated DSF window ranged from 2 to 2.4 W/m2/K in summer condition and 1.5 to 2.1 W/m^2/K in winter condition. When the opening was closed, the u_{DSF} value decreased by an average of 27% and 24% in summer and winter conditions, respectively.

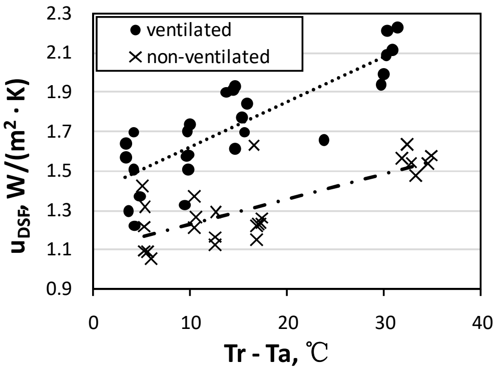

(a)

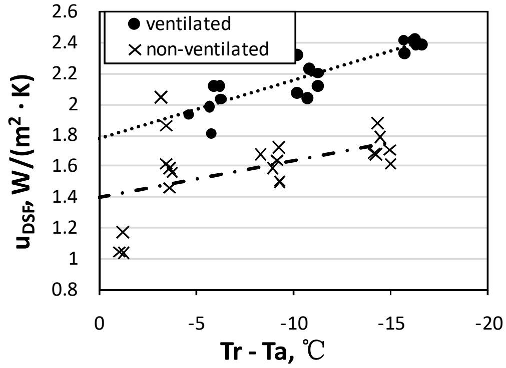

(b)

Figure 3. Heat transfer coefficient of the DSF window (u_{DSF}) at varied temperature difference with cavity ventilated or not (cavity width = 40 cm). a) winter mode; b) summer mode

Note that the averaged u_{DSF} under positive temperature difference (winter case, Figure 3a) was 16% smaller than the averaged u_{DSF} under negative temperature difference (summer case, Figure 3b) regardless the ventilation status. Similar phenomena could also be observed in other experiments. This indicates that downward draft along the double glazing in the cavity in summer is stronger than the upward buoyancy flow along the double glazing in summer. It might be explained by the direction of airflow and gravity. The upward draft in summer was against gravity and thus could be weakened while the downward draft could be strengthened by the gravity.

Impact of cavity width

Four cavity sizes were studied being 0cm, 10cm, 20 cm, and 40 cm with DSF operation in a ventilated mode and the u_{DSF} at cavity size of 0cm (pure double glazing) was measured as reference . Each case was repeated at least 3 times (Figure 4).

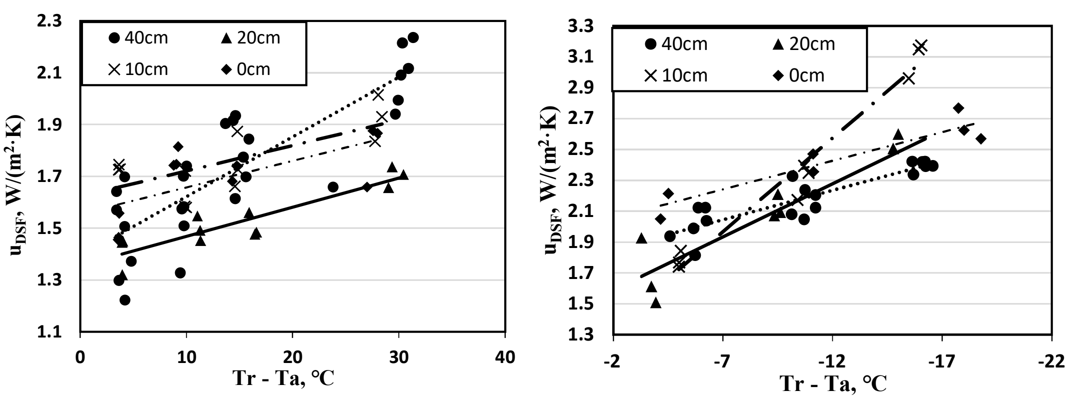

Figure 4. Heat transfer coefficient of the DSF window (u_{DSF}) at four cavity width and varied temperature difference. (left: winter mode; right: summer mode)

In the winter mode, u_{DSF} was lowest at cavity width = 20 cm indicating the existence of an optimal cavity width between 10 cm and 40 cm for the lowest heat transfer coefficient given the range of the temperature difference. A similar phenomenon, however, was not observed in the summer case. The DSF had better insulation when the cavity was wider at high outdoor temperature while it had better insulation when the cavity was narrower at low outdoor temperature. Although u_{DSF} decreased in general with the decrease of the temperature, the decreasing rates varied for different cavity width and different season. In the summer mode, the impact of temperature difference tended to disappear as the width decreased while in the winter mode the impact of temperature difference was stronger for the narrower cavity. The results indicate that the cavity width is an important factor to the insulation performance but its influence is dependent on the operation season and the outdoor temperature.

CONCLUSION

The heat transfer coefficient of a DSF window was measured at different cavity width and at varied temperature in the absence of solar radiation. The results showed that DSF has better insulation than the double glazing especially with closed cavity. All the studied factors (ventilation mode, cavity width, and outdoor temperature) had influence on the heat transfer coefficient of the DSF window and such influence could be season related. Measurements confirmed the existence of optimal width in winter for the best insulation.

ACKNOWLEDGEMENT

This work was supported by the National Natural Science Ffoundation of China (Grant No.51678518).

REFERENCES

Bueno, B. and M. Street, et al. (2017). A co-simulation modelling approach for the assessment of a ventilated double-skin complex fenestration system coupled with a compact fan-coil unit. Energy and Buildings 151: 18-27.

Chow, T. and C. Li, et al. (2010). Innovative solar windows for cooling-demand climate." Solar Energy Materials and Solar Cells 94 (2): 212-220.

Ghaffarianhoseini, A. and A. Ghaffarianhoseini, et al. (2016). Exploring the advantages and challenges of double-skin façades (DSFs). Renewable and Sustainable Energy Reviews 60: 1052-1065.

He, G. and J. Xu, et al. (2016). Prediction of solar heat gain of double skin facade windows. Building Simulation9 (4): 399-409.

Kapsis, K. and A. K. Athienitis (2015). A study of the potential benefits of semi-transparent photovoltaics in commercial buildings. Solar Energy 115: 120-132.

Li, Y. and J. Darkwa, et al. (2017). Heat transfer analysis of an integrated double skin façade and phase change material blind system. Building and Environment 125: 111-121.

Luo, Y. and L. Zhang, et al. (2017). A comparative study on thermal performance evaluation of a new double skin façade system integrated with photovoltaic blinds. Applied Energy 199: 281-293.

Peng, J. and L. Lu, et al. (2015). Comparative study of the thermal and power performances of a semi-transparent photovoltaic façade under different ventilation modes. Applied Energy 138: 572-583.

Poirazis H (2006). Double skin facades: A literature review. A Report of IEA SHC Task 34, ECBCS Annex 43. Lund University, Sweden.

Pomponi, F. and B. D'Amico (2017). Holistic study of a timber double skin façade: Whole life carbon emissions and structural optimisation. Building and Environment 124: 42-56.

Shen, C. and X. Li (2016). Thermal performance of double skin façade with built-in pipes utilizing evaporative cooling water in cooling season. Solar Energy 137: 55-65.